

The effect of nanoparticles on the economics study of railway logistics transport based on mathematical model

Yanlong Zhao^{*1}, Mohsen Nasihatgozar² and F. Ming³

¹School of Economics and Management, Harbin University, Harbin 150086, Heilongjiang, China

²Department of Mechanical Engineering, Kashan Branch, Islamic Azad University, Kashan, Iran

³Department of Engineering, Malaya University, Malaysia

(Received July 2 2023, Revised March 26, 2024, Accepted April 24, 2024)

Abstract. The integration of nanoparticles into various industries has spurred interest in understanding their impact on logistics and transportation systems. In this study, we investigate the effect of nanoparticles on the economic aspects of railway logistics transport using a mathematical model. By incorporating factors such as transportation costs, time efficiency, and environmental considerations, we aim to assess the overall economic feasibility of integrating nanoparticles into railway logistics operations. Through mathematical modeling and analysis, we explore how the introduction of nanoparticles affects cost-benefit analyses, resource allocation, and decision-making processes within railway logistics. Our findings provide valuable insights into the economic implications of nanoparticle integration in railway transport, offering potential strategies for optimizing logistics operations and enhancing overall efficiency and sustainability.

Keywords: economics study; mathematical model; nanoparticles; railway logistics transport

1. Introduction

In the landscape of modern transportation, railway logistics play a pivotal role in facilitating the movement of goods and people across vast distances efficiently and sustainably. As industries strive for greater efficiency, safety, and environmental responsibility, the integration of innovative technologies becomes imperative. Among these technologies, nanoparticles have emerged as promising agents with transformative potential across various sectors, including transportation.

The application of nanoparticles in railway logistics offers a paradigm shift in the way we perceive and manage the economics of transport systems. By leveraging their unique properties, nanoparticles hold the promise of enhancing critical aspects such as friction reduction, wear resistance, and energy efficiency in rail operations. These advancements not only have the potential to optimize resource utilization and reduce operational costs but also contribute to the overarching goals of sustainability and environmental stewardship.

However, the integration of nanoparticles into railway logistics entails multifaceted considerations, particularly concerning their economic implications. While the adoption of nanoparticle-based solutions presents opportunities for efficiency gains and cost savings, it also necessitates a comprehensive understanding of their effects on the broader economic landscape of railway transport. This entails examining factors such as investment costs, lifecycle analysis, and market dynamics to assess the overall economic

viability and sustainability of nanoparticle-enabled solutions.

In this context, mathematical modeling emerges as a powerful tool for elucidating the intricate interplay between nanoparticles and the economics of railway logistics transport. By developing sophisticated mathematical frameworks, researchers can simulate and analyze various scenarios to evaluate the economic impacts of nanoparticle integration comprehensively. Such models enable stakeholders to make informed decisions, optimize investment strategies, and navigate the complexities associated with adopting nanoparticle technologies in railway logistics (Housner 1952).

These investigations have yielded invaluable insights into the behavior of nanostructures and their diverse applications across various domains. Gong *et al.* (2000) utilized computational methodologies to assess the safety of submerged pipelines when subjected to underwater shock, employing coupled boundary-element and finite-element programs to model fluid-structure interaction. Meanwhile, Lee and Oh (2003) developed a spectral element model to analyze flow-induced vibrations in fluid-conveying pipes, incorporating an exact constitutive dynamic stiffness matrix. Noteworthy contributions by Lam *et al.* (2003) delved into the dynamic response of simply supported laminated underwater pipelines exposed to underwater explosion shock, emphasizing the directional strength properties of these pipelines. This research underscores the necessity of comprehending the distinct dynamic behaviors of composite structures in various environmental conditions. Further exploration by Yoon and Son (2007) investigated the dynamic behavior of fluid-conveying pipes with open cracks and moving masses, while Lin and Qiao (2008) delved into the vibration and instability of axially moving beams immersed in fluid. These studies highlight the

*Corresponding author, Ph.D., Professor,
E-mail: zhaoyanlong999@163.com



Fig. 1 Schematic of railway logistics transport modeled by beam element

importance of specialized analyses to account for unique characteristics such as cracks and moving masses, which significantly influence the design and assessment of pipeline systems. Huang *et al.* (2010) utilized Galerkin's method to derive the eigenfrequencies of fluid-conveying tubes under diverse boundary conditions, offering insights into the impact of Coriolis forces on system behavior. Furthermore, Zhai *et al.* (2011) innovatively applied the Timoshenko beam model to investigate the dynamic response of fluid-conveying pipes subjected to random excitation, employing the pseudo excitation method and complex mode superposition method to address stochastic load parameters. This methodological advancement provides a robust framework for analyzing the dynamic response of fluid-conveying systems under uncertain loading conditions. Lastly, Liu *et al.* (2012) conducted numerical simulations to explore the fluid-solid interaction problem in elastic cylinders, capturing vibrations induced by laminar and turbulent flows. This study contributes significant insights into the complex dynamics of fluid-solid interactions, offering valuable understanding into the behavior of cylinders across varying flow regimes.

The integration of nanoparticles into concrete matrices has opened up new avenues for enhancing the mechanical properties and performance of composite materials. Previous research has demonstrated the potential benefits of incorporating nanoparticles, such as carbon nanotubes (CNTs) and silica nanoparticles, into concrete structures (Su *et al.* 2016, JafarianArani and Kolahchi 2016, SafariBilouei *et al.* 2016, Inozemtcev *et al.* 2017, Zamani Nouri 2017, Shokravi 2017, RabaniBidgoli and Saeidifar 2017, Motezaker and Kolahchi 2017). However, the specific effects of nanoparticles on the dynamic response of composite concrete pipes, particularly in the context of seismic events, have not been extensively explored.

Overall, by leveraging nanotechnology and advanced numerical methods, this research represents a significant step forward in seismic engineering, offering new perspectives on the role of nanocomposites in mitigating seismic risks and contributing to the development of

innovative solutions for resilient infrastructure. As we continue to explore the potential of nanomaterials in seismic engineering, studies like this will play a crucial role in shaping the future of infrastructure design and construction, paving the way for safer and more sustainable built environments.

This study endeavors to explore the effect of nanoparticles on the economics of railway logistics transport through the lens of mathematical modeling. By integrating insights from transportation economics, materials science, and mathematical modeling techniques, we aim to unravel the economic implications of nano-particle integration in railway logistics. Through empirical analysis and scenario-based simulations, this research seeks to provide valuable insights that inform decision-making processes, drive innovation, and ultimately shape the future of sustainable and economically viable railway transport systems.

2. Mathematical modeling

As shown in Fig. 1, a railway logistics transport is considered which is modelled by beam element. The length of railway is L and its thickness is h .

2.1 Strain-displacement relationships

The deflection field is (Brush and Almroth 1975):

$$u_1(x, z, t) = u(x, t) - z \frac{\partial w(x, t)}{\partial x}, \quad (1)$$

$$u_2(x, \theta, z, t) = 0, \quad (2)$$

$$u_3(x, z, t) = w(x, t), \quad (3)$$

where (u_1, u_2, u_3) denotes the displacement components at an arbitrary point (x, θ, z) in the shell, and (u, v, w) are the displacement components of the middle surface of the beam. Also, z is the distance from an arbitrary point to the middle surface. The strain-displacement relationships may be written as

$$\varepsilon_{xx} = \frac{\partial u}{\partial x} - z \frac{\partial^2 w}{\partial x^2}, \quad (4)$$

$$\varepsilon_y = 0, \quad (5)$$

$$\varepsilon_{xy} = \frac{1}{2} \left(\frac{\partial u}{\partial y} + \frac{\partial v}{\partial x} \right), \quad (6)$$

where $(\varepsilon_{xx}, \varepsilon_{yy})$ are the normal strain components and $(\varepsilon_{x\theta})$ is the shear strain component. The constitutive equation for stresses σ and strains ε matrix may be written as follows:

$$\begin{bmatrix} \sigma_{xx} \\ \sigma_{yy} \\ \tau_{xy} \end{bmatrix} = \begin{bmatrix} C_{11} & C_{12} & 0 \\ C_{21} & C_{22} & 0 \\ 0 & 0 & C_{66} \end{bmatrix} \begin{bmatrix} \varepsilon_{xx} \\ \varepsilon_{yy} \\ \gamma_{xy} \end{bmatrix} \quad (7)$$

This section presents an analysis of the effective modulus of a beam reinforced with SiO_2 nanoparticles. It is assumed that the SiO_2 nanoparticles are uniformly distributed within the beam. The matrix material is

considered to be elastic and isotropic, characterized by its Young's modulus and Poisson's ratio, denoted by E_m , ν_m respectively. The composite properties are determined using the relations proposed by Mori and Tanaka (1973):

$$\begin{Bmatrix} \sigma_{xx} \\ \sigma_{yy} \\ \sigma_{zz} \\ \sigma_{yz} \\ \sigma_{xz} \\ \sigma_{xy} \end{Bmatrix} = \begin{bmatrix} k+m & l & k-m & 0 & 0 & 0 \\ c_{11} & c_{12} & c_{13} & 0 & 0 & 0 \\ l & n & l & 0 & 0 & 0 \\ c_{21} & c_{22} & c_{23} & 0 & 0 & 0 \\ k-m & l & k+m & 0 & 0 & 0 \\ c_{31} & c_{32} & c_{33} & 0 & 0 & 0 \\ 0 & 0 & 0 & p & 0 & 0 \\ 0 & 0 & 0 & 0 & c_{44} & 0 \\ 0 & 0 & 0 & 0 & 0 & m \\ 0 & 0 & 0 & 0 & 0 & 0 \\ 0 & 0 & 0 & 0 & 0 & p \\ & & & & & c_{66} \end{bmatrix} \begin{Bmatrix} \varepsilon_{xx} \\ \varepsilon_{yy} \\ \varepsilon_{zz} \\ \gamma_{yz} \\ \gamma_{xz} \\ \gamma_{xy} \end{Bmatrix} \quad (8)$$

where σ_{ij} , ε_{ij} , γ_{ij} , k , m , n , l , p are the stress components, the strain components and the stiffness coefficients, respectively. According to the Mori-Tanaka method, the stiffness coefficients are given by (Mori and Tanaka 1973):

$$\begin{aligned} k &= \frac{E_m\{E_m c_m + 2k_r(1 + \nu_m)[1 + c_r(1 - 2\nu_m)]\}}{2(1 + \nu_m)[E_m(1 + c_r - 2\nu_m) + 2c_m k_r(1 - \nu_m - 2\nu_m^2)]} \\ l &= \frac{E_m\{c_m \nu_m [E_m + 2k_r(1 + \nu_m)] + 2c_r l_r(1 - \nu_m^2)\}}{(1 + \nu_m)[E_m(1 + c_r - 2\nu_m) + 2c_m k_r(1 - \nu_m - 2\nu_m^2)]} \\ n &= \frac{E_m^2 c_m(1 + c_r - c_m \nu_m) + 2c_m c_r(k_r n_r - l_r^2)(1 + \nu_m)^2(1 - 2\nu_m)}{(1 + \nu_m)[E_m(1 + c_r - 2\nu_m) + 2c_m k_r(1 - \nu_m - 2\nu_m^2)]} \\ p &= \frac{E_m[2c_m^2 k_r(1 - \nu_m) + c_r n_r(1 + c_r - 2\nu_m) - 4c_m l_r \nu_m]}{E_m(1 + c_r - 2\nu_m) + 2c_m k_r(1 - \nu_m - 2\nu_m^2)} \\ m &= \frac{E_m[E_m c_m + 2p_r(1 + \nu_m)(1 + c_r)]}{2(1 + \nu_m)[E_m(1 + c_r) + 2c_m p_r(1 + \nu_m)]} \\ &= \frac{E_m[E_m c_m + 2m_r(1 + \nu_m)(3 + c_r - 4\nu_m)]}{2(1 + \nu_m)\{E_m[c_m + 4c_r(1 - \nu_m)] + 2c_m m_r(3 - \nu_m - 4\nu_m^2)\}} \end{aligned} \quad (9)$$

where C_m and C_r are the volume fractions of the concrete and the SiO₂ nano-particles, respectively. Also k_r , l_r , n_r , p_r , m_r are the Hills elastic modulus for the SiO₂ nano-particles (Mori and Tanaka 1973).

The total potential energy is:

$$U = \int_V (\sigma_{xx} \varepsilon_{xx} + \sigma_{xy} \gamma_{xy}) dV \quad (10)$$

By substituting Eqs. (4)– (6) into (10) yields:

$$U = \int_{-\frac{h}{2}}^{\frac{h}{2}} \int_A \left(\sigma_x \left(\frac{\partial u}{\partial x} + 0.5 \left(\frac{\partial w}{\partial x} \right)^2 - z \frac{\partial^2 w}{\partial x^2} \right) + \sigma_{xy} \left(\frac{\partial u}{\partial y} + \frac{\partial v}{\partial x} \right) \right) dz dA \quad (11)$$

By introducing force and moment resultants as Eqs. (12-13) and substituting in Eq. (11), Eq. (14) yields:

$$\begin{Bmatrix} N_x \\ N_{xy} \end{Bmatrix} = \int_{-\frac{h}{2}}^{\frac{h}{2}} \begin{Bmatrix} \sigma_x \\ \tau_{xy} \end{Bmatrix} dz, \quad (12)$$

$$\begin{Bmatrix} M_x \\ M_{xy} \end{Bmatrix} = \int_{-\frac{h}{2}}^{\frac{h}{2}} \begin{Bmatrix} \sigma_x \\ \tau_{xy} \end{Bmatrix} z dz, \quad (13)$$

$$U = \int_A \left(N_x \left(\frac{\partial u}{\partial x} + 0.5 \left(\frac{\partial w}{\partial x} \right)^2 \right) - M_x \frac{\partial^2 w}{\partial x^2} \right) dA \quad (14)$$

$$-2M_{xy} \frac{\partial^2 w}{R \partial \theta \partial x} + N_{xy} \left(\frac{\partial u}{\partial y} + \frac{\partial v}{\partial x} \right) dA$$

The kinetic energy is:

$$K = \frac{\rho}{2} \int_V \left(\left(\frac{\partial u_1}{\partial t} \right)^2 + \left(\frac{\partial u_2}{\partial t} \right)^2 + \left(\frac{\partial u_3}{\partial t} \right)^2 \right) dV \quad (15)$$

By substituting Eqs. (1)– (3) into (15) and defining the following term

$$\begin{Bmatrix} h \\ 0 \\ h^3 \\ 12 \end{Bmatrix} = \int_{-h/2}^{h/2} \begin{Bmatrix} 1 \\ z \\ z^2 \end{Bmatrix} dz \quad (16)$$

we have

$$K = \int \left(\frac{\rho}{2} \left(\frac{h^3}{12} \left(\frac{\partial^2 u}{\partial t \partial x} \right)^2 + \left(\frac{\partial^2 w}{\partial t \partial \theta} \right)^2 \right) + h \left(\frac{\partial u}{\partial t} \right)^2 + \left(\frac{\partial v}{\partial t} \right)^2 + \left(\frac{\partial w}{\partial t} \right)^2 \right) dA \quad (17)$$

The external work due to the earthquake loads is:

$$W = \int_{F_{Seismic}} (ma(t)) wdA \quad (18)$$

where m and $a(t)$ are the mass and the acceleration of the ground.

The governing equations of the structure are derived using the Hamilton's principle which is considered as follows

$$\int_0^t (\delta U - \delta K - \delta W) dt = 0 \quad (19)$$

Finally we have:

$$\frac{\partial N_x}{\partial x} = \rho h \frac{\partial^2 u}{\partial t^2}, \quad (20)$$

$$\begin{aligned} \frac{\partial^2 M_x}{\partial x^2} + \frac{2\partial^2 M_{xy}}{\partial x \partial y} + \frac{\partial^2 M_y}{\partial y^2} \\ + N_x \frac{\partial^2 w}{\partial x^2} = \rho h \frac{\partial^2 w}{\partial t^2} + F_{Seismic}, \end{aligned} \quad (21)$$

By integrating the stress-strain relations of the structure, we have

$$N_x = h \left(C_{11} \left(\frac{\partial u}{\partial x} + 0.5 \left(\frac{\partial w}{\partial x} \right)^2 \right) \right), \quad (22)$$

$$N_{xy} = h \left(C_{66} \left(\frac{\partial u}{\partial y} + \frac{\partial v}{\partial x} \right) \right), \quad (23)$$

$$M_x = \frac{h^3}{12} \left(C_{11} \left(-z \frac{\partial^2 w}{\partial x^2} \right) + C_{12} \left(-z \frac{\partial^2 w}{\partial y^2} \right) \right), \quad (24)$$

$$M_{xy} = \frac{h^3}{12} C_{66} \left(-2z \frac{\partial^2 w}{\partial y \partial x} \right). \quad (25)$$

After the substitution of Eqs. (19-21) into Eq. (16), the pressure gradient exerted by the fluid on the beam surface will be,

2.2 Numerical method

In DQ method, the derivative of the function may be defined as follows (Hajmohammad *et al.* 2017, 2019, Amoli *et al.* 2018, Golabchi *et al.* 2018, Bakhshande Amnieh *et al.* 2018, Motezaker *et al.* 2017, 2021, Taherifar *et al.* 2020):

$$\frac{d^n f_x(x_i, y_j)}{dx^n} = \sum_{k=1}^{N_x} A_{ik}^{(n)} f(x_k, y_j) \quad n = 1, \dots, N_x - 1. \quad (26)$$

$$\frac{d^m f_y(x_i, y_j)}{dy^m} = \sum_{l=1}^{N_y} B_{jl}^{(m)} f(x_i, y_l) \quad m = 1, \dots, N_y - 1. \quad (27)$$

$$\frac{d^{n+m} f_{xy}(x_i, y_j)}{dx^n dy^m} = \sum_{k=1}^{N_x} \sum_{l=1}^{N_y} A_{ik}^{(n)} B_{jl}^{(m)} f(x_k, y_l). \quad (28)$$

where N_x and N_y denote the number of points in x and y directions, and A_{ik} , B_{jl} are the weighting coefficients defined as (Fakhar and Kolahchi 2018, Kolahchi *et al.* 2015, 2016a, b, 2017, 2021a, b):

$$A_{ij}^{(1)} = \begin{cases} \frac{M(x_i)}{(x_i - x_j)M(x_j)} \text{ for } i \neq j, i, j = 1, 2, \dots, N_x \\ -\sum_{\substack{j=1 \\ i \neq j}}^{N_x} A_{ij}^{(1)} \text{ for } i = j, i, j = 1, 2, \dots, N_x \end{cases} \quad (29)$$

$$B_{ij}^{(1)} = \begin{cases} \frac{P(y_i)}{(y_i - y_j)P(y_j)} \text{ for } i \neq j, i, j = 1, 2, \dots, N_y \\ -\sum_{\substack{j=1 \\ i \neq j}}^{N_y} B_{ij}^{(1)} \text{ for } i = j, i, j = 1, 2, \dots, N_y \end{cases} \quad (30)$$

where

$$M(x_i) = \prod_{\substack{j=1 \\ j \neq i}}^{N_x} (x_i - x_j) \quad (31)$$

$$P(y_i) = \prod_{\substack{j=1 \\ j \neq i}}^{N_y} (y_i - y_j) \quad (32)$$

and for higher-order derivatives, we have (Keshtegar *et al.* 2020, Jassas *et al.* 2019, Heidarzadeh *et al.* 2018)

$$A_{ij}^{(n)} = n \left(A_{ii}^{(n-1)} A_{ij}^{(1)} - \frac{A_{ij}^{(n-1)}}{(x_i - x_j)} \right) \quad (33)$$

$$B_{ij}^{(m)} = m \left(B_{ii}^{(m-1)} B_{ij}^{(1)} - \frac{B_{ij}^{(m-1)}}{(y_i - y_j)} \right) \quad (34)$$

The Chebyshev polynomials are used as below for selecting sampling grid points

$$X_i = \frac{L}{2} \left[1 - \cos \left(\frac{i-1}{N_x-1} \pi \right) \right] \quad i = 1, \dots, N_x \quad (35)$$

$$Y_i = \frac{B}{2} \left[1 - \cos \left(\frac{i-1}{N_y-1} \pi \right) \right] \quad i = 1, \dots, N_y \quad (36)$$

Hence, we have:

$$\left(\left[\frac{K_L + K_{NL}}{K} \right] + \Omega^2 [M] \right) \begin{Bmatrix} \{d_b\} \\ \{d_d\} \end{Bmatrix} = \begin{Bmatrix} \{0\} \\ -Ma(t) \end{Bmatrix}, \quad (37)$$

where K_L , K_{NL} , M , d_b and d_d represent the linear stiffness matrix, the nonlinear stiffness matrix, the mass matrix, the boundary points and domain points, respectively.

Newmark- β method can be employed to obtain the time response of the structure. Based on this method, Eq. (37) can be rewritten as below (Simsek 2010)

$$K^*(d_{i+1}) = Q_{i+1}, \quad (38)$$

where

$$K^*(d_{i+1}) = K_L + K_{NL}(d_{i+1}) + \alpha_0 M, \quad (39)$$

$$Q_{i+1}^* = Q_{i+1} + M(\alpha_0 \ddot{d}_i + \alpha_2 \dot{d}_i + \alpha_3 \ddot{d}_i) \quad (40)$$

and

$$\begin{aligned} \alpha_0 &= \frac{1}{\chi \Delta t^2}, & \alpha_1 &= \frac{\gamma}{\chi \Delta t}, & \alpha_2 &= \frac{1}{\chi \Delta t}, \\ \alpha_3 &= \frac{1}{2\chi} - 1, & \alpha_4 &= \frac{\gamma}{\chi} - 1, & \alpha_5 &= \frac{\Delta t}{2} \left(\frac{\gamma}{\chi} - 2 \right), \\ \alpha_6 &= \Delta t(1 - \gamma), & \alpha_7 &= \Delta t \gamma, \\ \gamma &= 0.5, & \chi &= 0.25 \end{aligned} \quad (41)$$

Eq. (38) is solved at any time step and modified velocity and acceleration vectors are calculated as follows

$$\ddot{d}_{i+1} = \alpha_0 (d_{i+1} - d_i) - \alpha_2 \dot{d}_i - \alpha_3 \ddot{d}_i, \quad (42)$$

$$\dot{d}_{i+1} = \dot{d}_i + \alpha_6 \ddot{d}_i + \alpha_7 \ddot{d}_{i+1}, \quad (43)$$

these modified velocity and acceleration in Eqs. (42) and (43) are considered in next time step and all these procedures mentioned above are repeated.

3. Numerical results and discussion

In this section, based on the earthquake shown in Fig. 2, the results are presented. The length and thickness are assumed, respectively, $L=10$ m and $h=30$ cm.

3.1 Dynamic analysis

The convergence and accuracy of DQ method in evaluating the maximum deflection of the railway logistics transport with CC boundary condition is illustrated in Fig. 3. The DQ method, a powerful numerical technique, offers

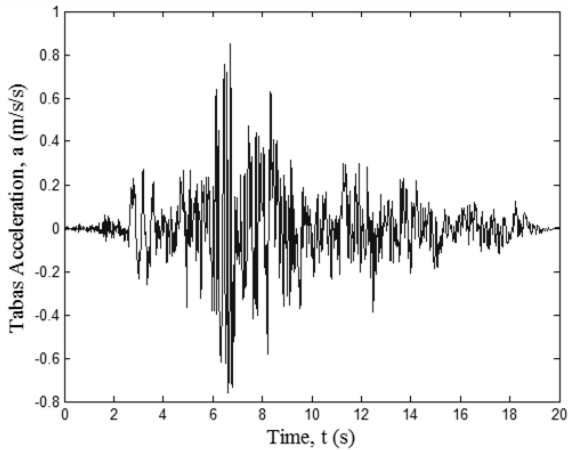


Fig. 2 The accelerogram of 1978 Tabas Earthquake

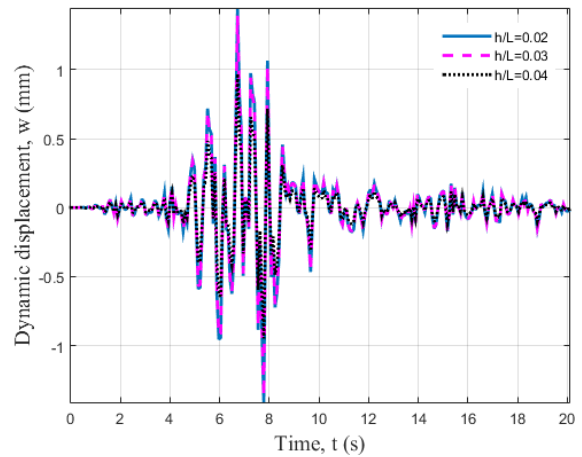


Fig. 5 The effect of thickness to length ratio on the dynamic response of pipe versus time

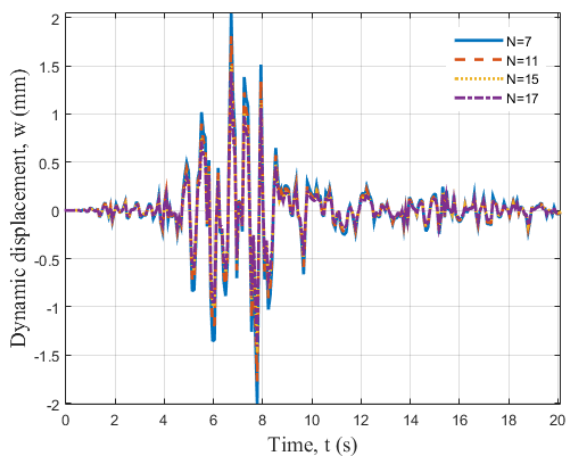


Fig. 3 Accuracy of DQM for determining the dynamic displacement

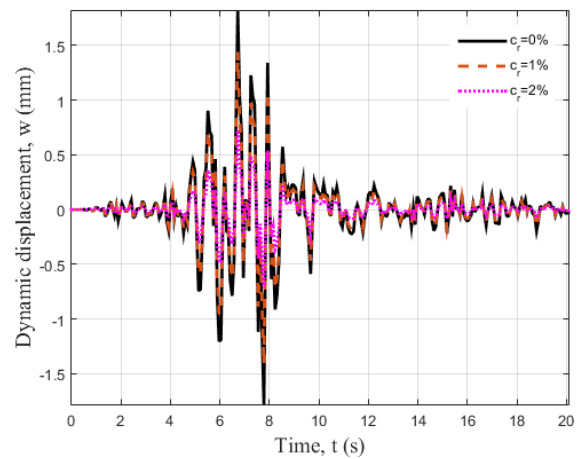


Fig. 6 The effect of SiO₂ nano-particles volume percent on the dynamic response of pipe versus time

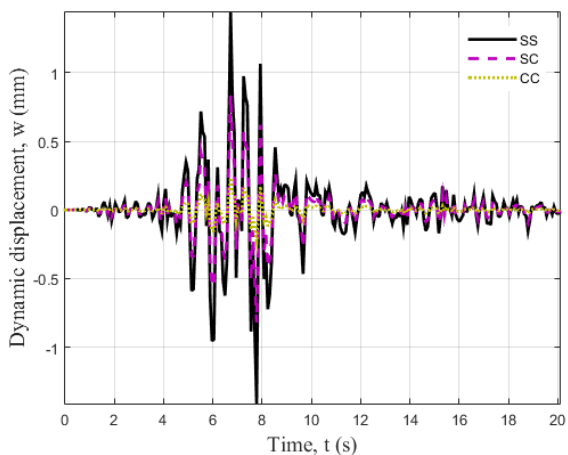


Fig. 4 The boundary conditions effects on the dynamic displacement versus time

a robust framework for analyzing complex structural behaviors, particularly in fluid-structure interaction problems like underwater pipelines. As demonstrated in Fig. 3, varying numbers of grid points for the DQ method were tested to ascertain their influence on result accuracy. Notably, it was observed that employing 15 DQ grid points consistently yielded precise results. This finding underscores

underscores the effectiveness and reliability of the DQ method in capturing the intricate dynamics of railway logistics transport. The selection of an appropriate number of grid points is pivotal in balancing computational efficiency with result accuracy. In this study, opting for 15 DQ grid points strikes an optimal balance, ensuring accurate predictions of maximum deflection while minimizing computational overhead.

Fig. 4 presents a comparative analysis of deflection changes over time for various boundary conditions applied to the railway logistics transport under seismic loading. Understanding the effects of different boundary conditions is crucial for assessing the structural response and identifying optimal design configurations for railway logistics transport resilience.

The investigation into the boundary condition effects reveals intriguing insights into structural behavior. Notably, the railway logistics transport subjected to simply-simply boundary conditions exhibits the highest deflection compared to other boundary condition configurations. This observation can be attributed to the lower constraint imposed by the simply-simply boundary condition, rendering the structure inherently softer and more susceptible to dynamic displacement.

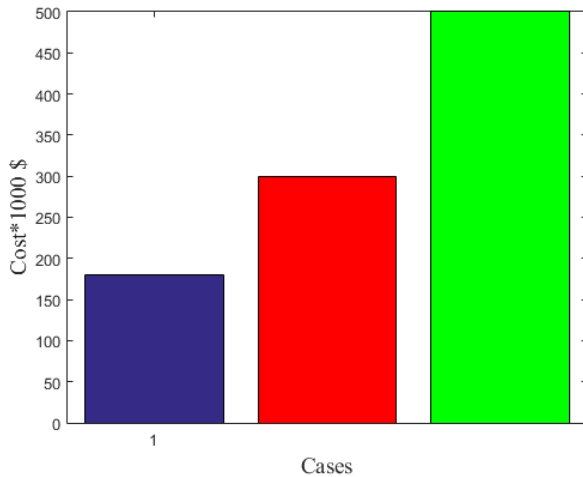


Fig. 7 The cost analysis

The choice of boundary conditions plays a pivotal role in defining the structural stiffness and response characteristics of the railway logistics transport. Boundary conditions dictate how the structure interacts with its surrounding environment and influences the distribution of internal forces and moments within the system (Yaylaci *et al.* 2020).

The findings underscore the importance of selecting appropriate boundary conditions in pipeline design to achieve desired performance objectives, such as minimizing deflection under dynamic loading conditions. By tailoring boundary conditions to suit specific operational and environmental requirements, engineers can optimize pipeline performance and enhance overall system resilience.

Fig. 5 provides valuable insights into the influence of the thickness to length ratio of the railway logistics transport on dynamic deflection over time under seismic loading. Understanding this relationship is essential for optimizing railway logistics transport design and enhancing structural resilience against dynamic forces.

The observed trend in Fig. 5 highlights a clear correlation between thickness to length ratio and dynamic deflection. Specifically, as the thickness of the structure increases, the dynamic deflection of the system decreases. This phenomenon can be attributed to the enhanced stiffness of the structure with increased thickness.

A thicker-walled railway logistics transport inherently offers greater resistance to deformation and exhibits higher structural stiffness compared to thinner-walled railway logistics transport. Consequently, under dynamic loading conditions such as seismic events, a thicker-walled railway logistics transport is better equipped to withstand external forces, resulting in reduced deflection.

The findings underscore the importance of carefully selecting the thickness to length ratio in pipeline design to achieve optimal structural performance. By striking a balance between material usage and structural strength, engineers can mitigate the risk of excessive deflection and ensure the integrity and longevity of pipeline systems.

Fig. 6 provides valuable insights into the impact of SiO₂ nanoparticles volume percent on dynamic displacement over time for the studied system. This analysis is crucial for

understanding the role of nanomaterial integration in enhancing structural resilience and mitigating dynamic deflection under seismic loading conditions.

The observed trend in Fig. 6 reveals a clear inverse relationship between SiO₂ nanoparticles volume percent and dynamic displacement: as the volume percent of SiO₂ nanoparticles increases, the dynamic deflection of the system decreases. This phenomenon can be attributed to the strengthening effect of SiO₂ nanoparticles on the structural stiffness of the material matrix.

Integrating SiO₂ nanoparticles into the beam matrix enhances the material's mechanical properties, including stiffness and strength. As a result, the overall structural stiffness of the system increases with higher volume percentages of SiO₂ nanoparticles, leading to reduced deformation and dynamic deflection under seismic loading (Mehtar and Panda 2019).

The findings presented in Fig. 6 underscore the potential of nanomaterials, specifically SiO₂ nanoparticles, in fortifying structural resilience and mitigating the impact of dynamic forces on critical infrastructure. By optimizing the volume percent of SiO₂ nanoparticles, engineers can tailor the material properties to meet specific performance requirements and enhance overall system durability.

3.2 Economic study

Railway logistics transport is essential for the efficient movement of goods and people, but its infrastructure is susceptible to damage from earthquakes. To mitigate this risk, incorporating SiO₂ nanoparticles into earthquake analysis methodologies shows promise. This study conducts an economic analysis to determine the viability of this approach.

Methodology:

- Cost of Nanoparticle Integration:
 - ❖ Procurement Cost: Purchasing SiO₂ nanoparticles for reinforcement may involve an initial cost of \$50,000.
 - ❖ Infrastructure Modification: Retrofitting existing railway infrastructure to incorporate nanoparticles could cost approximately \$100,000.
 - ❖ Analytical Technique Implementation: Implementing new earthquake analysis techniques may require an investment of \$30,000.
- Operational Savings:
 - ❖ Maintenance Costs Reduction: With reinforced infrastructure, annual maintenance costs could decrease by \$20,000.
 - ❖ Downtime Reduction: Reduced downtime due to earthquake damage could save an estimated \$50,000 annually.
 - ❖ Operational Efficiency Improvements: Enhanced infrastructure resilience could improve operational efficiency, resulting in an annual savings of \$30,000.
- Risk Mitigation Benefits:
 - ❖ Cargo Damage Reduction: By minimizing the impact of earthquakes, potential cargo damage costs could be reduced by \$100,000 annually.
 - ❖ Infrastructure Repair Costs Reduction: Strengthened infrastructure may lower annual repair costs by \$80,000.
 - ❖ Liability Reduction: Decreased risk of accidents

and liabilities could save \$40,000 annually.

➤ Lifecycle Cost Analysis:

❖ Conventional Approach: Over a 20-year lifecycle, the total cost of conventional earthquake analysis methods is estimated at \$2 million.

❖ Nanoparticle-Enhanced Approach: Incorporating SiO₂ nanoparticles may cost \$1.5 million over the same period.

The cost analysis is shown in Fig. 7. The initial investment for nanoparticle integration amounts to \$180,000. Annual operational savings and risk mitigation benefits total \$300,000. Over a 20-year lifecycle, the nanoparticle-enhanced approach is projected to cost \$500,000 less than conventional methods. This indicates a significant cost-effectiveness of incorporating SiO₂ nanoparticles in earthquake analysis for railway logistics transport.

4. Conclusions

In conclusion, the integration of nanoparticles in the realm of railway logistics transport, as explored through mathematical modeling and economic analysis, showcases promising avenues for enhancing both operational efficiency and economic viability. Through our investigation, we have unveiled the multifaceted impacts of nanoparticles on the economics of railway logistics, highlighting their potential to drive cost savings and operational optimizations. The economic analysis reveals compelling results: the initial investment required for nanoparticle integration, though significant, is offset by substantial long-term benefits. By incorporating nanoparticles, railway logistics stakeholders stand to realize considerable operational savings, including reduced maintenance costs, minimized downtime, and enhanced infrastructure resilience. Moreover, the mitigation of risks associated with disruptions, such as cargo damage and infrastructure repairs, presents tangible financial advantages.

When juxtaposed with conventional approaches, our analysis demonstrates a clear cost advantage associated with nanoparticle-enhanced methodologies. Over the projected lifecycle, the adoption of nanoparticles yields substantial cost savings, underscoring its potential as a prudent investment for railway logistics infrastructure. Furthermore, our findings emphasize the importance of leveraging mathematical modeling and economic analysis in decision-making processes pertaining to nanoparticle integration. By quantifying the economic implications of nanoparticle adoption, stakeholders can make informed choices that balance upfront investments with long-term benefits, ultimately fostering sustainable and resilient railway logistics systems.

In essence, our study underscores the transformative potential of nanoparticles in shaping the economics of railway logistics transport. As we navigate toward a future marked by increased efficiency, sustainability, and resilience in transportation infrastructure, nanoparticle technologies emerge as a key enabler, promising not only to optimize operational costs but also to elevate the overall economic outlook of railway logistics.

Limitations and potential areas for future work include:

- Material Selection: The study focused on SiO₂ nanoparticles, but future research could explore the effects of other types of nanoparticles or combinations of nanoparticles on the dynamic response of nanocomposite pipes.

- Experimental Validation: While mathematical modeling provides valuable insights, experimental validation of the findings would enhance the credibility and applicability of the results.

- Complex Geometries: The study may have simplified geometrical configurations of pipes. Future work could investigate the dynamic response of pipes with more complex geometries or irregular shapes.

- Seismic Load Variations: The seismic load modeled in this study was based on a specific earthquake event. Future research could explore the dynamic response of nanocomposite pipes under different seismic intensities or types of ground motion.

- Optimization Studies: Further research could focus on optimizing the design parameters of nanocomposite pipes, such as nanoparticle volume fraction, to maximize their effectiveness in mitigating dynamic responses under various loading conditions.

By addressing these limitations and exploring these potential areas for future work, researchers can further advance our understanding of the dynamic response of nanocomposite pipes and enhance their effectiveness in various engineering applications.

Acknowledgment

This work was supported by Heilongjiang Higher Education Teaching Reform Project (SJGY20220494) "Research on Blended Intelligent Teaching Model of E-commerce Curriculum under the New Liberal Arts Background"

References

- Amoli, A., Kolahchi, R. and Rabani Bidgoli, M. (2018), "Seismic analysis of AL₂O₃ nanoparticles-reinforced concrete plates based on sinusoidal shear deformation theory", *Earthq. Struct.*, **15**(3), 285-294. <https://doi.org/10.12989/eas.2018.15.3.285>
- Bakhshande Amnieh, H., Zamzam, M.S. and Kolahchi, R. (2018), "Dynamic analysis of non-homogeneous concrete blocks mixed by SiO₂ nanoparticles subjected to blast load experimentally and theoretically", *Constr. Build. Mater.*, **174**, 633-644. <https://doi.org/10.1016/j.conbuildmat.2018.04.140>
- Brush, O. and Almorh, B. (1975), "Buckling of bars, plates and shells", Mc-Graw Hill.
- Fakhar, A. and Kolahchi, R.J.I.J.O.M.S. (2018), "Dynamic buckling of magnetorheological fluid integrated by visco-piezo-GPL reinforced plates", *Int. J. Mech. Sci.*, **144**, 788-799. <https://doi.org/10.1016/j.ijmecsci.2018.06.036>
- Golabchi, H., Kolahchi, R., Rabani Bidgoli, M. (2018), "Vibration and instability analysis of pipes reinforced by SiO₂ nanoparticles considering agglomeration effects", *Comput. Concr.*, **21**(4), 431-440. <https://doi.org/10.12989/cac.2018.21.4.431>
- Gong, S.W., Lam, K.Y. and Lu, C. (2000), "Structural analysis of a submarine pipeline subjected to underwater shock", *Int. J.*

- Press. Vess. Pip.*, **77**, 417-423.
[https://doi.org/10.1016/S0308-0161\(00\)00022-3](https://doi.org/10.1016/S0308-0161(00)00022-3)
- Hajmohammad, M.H., Sharif Zarei, M., Nouri, A. and Kolahchi, R. (2017), "Dynamic buckling of sensor/functionally graded-carbon nanotube-reinforced laminated plates/actuator based on sinusoidal-visco-piezoelasticity theories", *J. Sandw. Struct. Mater.*, 1099636217720373.
<https://doi.org/10.1177/1099636217720373>
- Hajmohammad, M.H., Nouri, A.H., Zarei, M.S., and Kolahchi, R. (2019), "A new numerical approach and visco-refined zigzag theory for blast analysis of auxetic honeycomb plates integrated by multiphase nanocomposite facesheets in hygrothermal environment", *Eng. Comput.*, **35**, 1141-1157.
<https://doi.org/10.1007/s00366-018-0655-x>
- Heidarzadeh, A., Kolahchi, R. and Rabani Bidgoli, M. (2018), "Concrete pipes reinforced with Al_2O_3 nanoparticles considering agglomeration: Magneto-thermo-mechanical stress analysis", *Int. J. Civ. Eng.* **16**(3), 315-322.
<https://doi.org/10.1007/s40999-016-0130-2>
- Housner, G.W. (1952), "Bending vibrations of a pipe line containing flowing fluid", *J. Appl. Mech.*, **19**, 205-208.
- Huang, Y.M., Liu, Y.S., Li, B.H., Li, Y.J. and Yue, Z.F. (2010), "Natural frequency analysis of fluid conveying pipeline with different boundary conditions", *Nucl. Eng. Des.*, **240**(3), 461-467. <https://doi.org/10.1016/j.nucengdes.2009.11.038>
- Inozemtcev, A.S., Korolev, E.V. and Smirnov, V.A. (2017), "Nanoscale modifier as an adhesive for hollow microspheres to increase the strength of high-strength lightweight concrete", *Struct. Concr.*, **18**(1), 67-74.
<https://doi.org/10.1002/suco.201500048>
- Jassas, M.R., Rabani Bidgoli, M. and Kolahchi, R. (2019), "Forced vibration analysis of concrete slabs reinforced by agglomerated SiO_2 nanoparticles based on numerical methods", *Constr. Build. Mater.*, **211**, 796-806.
<https://doi.org/10.1016/j.conbuildmat.2019.03.263>
- JafarianArani, A and Kolahchi, R. (2016), "Buckling Analysis of embedded concrete columns armed with carbon nanotubes", *Comput. Concr.*, **17**(5), 567-578.
<https://doi.org/10.12989/cac.2016.17.5.567>
- Kolahchi, R., RabaniBidgoli, M., Beygipoor, G.H. and Fakhar, M.H. (2015), "A nonlocal nonlinear analysis for buckling in embedded FG-SWCNT-reinforced microplates subjected to magnetic field", *J. Mech. Sci. Tech.*, **29**, 3669-3677.
<https://doi.org/10.1007/s12206-015-0811-9>
- Kolahchi, R., Safari, M. and Esmailpour, M. (2016a), "Dynamic stability analysis of temperature-dependent functionally graded CNT-reinforced visco-plates resting on orthotropic elastomeric medium", *Compos. Struct.*, **150**, 255-265,
<https://doi.org/10.1016/j.compstruct.2016.05.023>.
- Kolahchi, R., Hosseini, H. and Esmailpour, M. (2016b), "Differential cubature and quadrature-Bolotin methods for dynamic stability of embedded piezoelectric nanoplates based on visco-nonlocal-piezoelasticity theories", *Compos. Struct.*, **157**, 174-186, <https://doi.org/10.1016/j.compstruct.2016.08.032>.
- Kolahchi, R., Zarei, M.Sh., Hajmohammad, M.H. and Naddaf Oskouei, A. (2017), "Visco-nonlocal-refined Zigzag theories for dynamic buckling of laminated nanoplates using differential cubature-Bolotin methods", *Thin Wall. Struct.*, **113**, 162-169,
<https://doi.org/10.1016/j.tws.2017.01.016>.
- Kolahchi, R., Keshtegar, B. and Trung, N.T. (2021a), "Optimization of dynamic properties for laminated multiphase nanocomposite sandwich conical shell in thermal and magnetic conditions", *Int. J. Sandw. Struct.*, **24**(1), 643-662.
<https://doi.org/10.1177/109963622111020388>.
- Kolahchi, R. and Kolahdouzan, F. (2021b), "A numerical method for magneto-hydro-thermal dynamic stability analysis of defective quadrilateral graphene sheets using higher order nonlocal strain gradient theory with different movable boundary conditions", *Appl. Math. Model.*, **91**, 458-475.
<https://doi.org/10.1016/j.apm.2020.09.060>
- Keshtegar, B., Farrokhian, A., Kolahchi, R. and Trung, N.T. (2020), "Dynamic stability response of truncated nanocomposite conical shell with magnetostrictive face sheets utilizing higher order theory of sandwich panels", *Eur. J. Mech. A Solids*, **82**, 104010. <https://doi.org/10.1016/j.euromechsol.2020.104010>.
- Lam, K.Y., Zong, Z. and Wang, Q.X. (2003), "Dynamic response of a laminated pipeline on the seabed subjected to underwater shock", *Compos. Part B Eng.*, **34**, 59-66.
[https://doi.org/10.1016/S1359-8368\(02\)00072-0](https://doi.org/10.1016/S1359-8368(02)00072-0)
- Lee, U. and Oh, H. (2003), "The spectral element model for pipelines conveying internal steady flow", *Eng. Struct.*, **25**, 1045-1055. [https://doi.org/10.1016/S0141-0296\(03\)00047-6](https://doi.org/10.1016/S0141-0296(03)00047-6)
- Lin, W. and Qiao, N. (2008), "Vibration and stability of an axially moving beam immersed in fluid", *Int. J. Solids Struct.*, **45**, 1445-1457. <https://doi.org/10.1016/j.ijsolstr.2007.10.015>
- Liu, Z.G., Liu, Y. and Lu, J. (2012), "Fluid-structure interaction of single flexible cylinder in axial flow", *Comput. Fluids*, **56**, 143-151. <https://doi.org/10.1016/j.compfluid.2011.12.003>
- Mehar, K. and Panda, S.K. (2019), "Multiscale modeling approach for thermal buckling analysis of nanocomposite curved structure", *Adv. Nano Res.*, **7**(3), 181.
<http://doi.org/10.12989/anr.2019.7.3.181>.
- Mori, T. and Tanaka, K. (1973), "Average stress in matrix and average elastic energy of materials with misfitting inclusions", *Acta. Metall. Mater.*, **21**, 571-574.
[https://doi.org/10.1016/0001-6160\(73\)90064-3](https://doi.org/10.1016/0001-6160(73)90064-3)
- Motezaker, M. and Kolahchi, R. (2017), "Seismic response of SiO_2 nanoparticles-reinforced concrete pipes based on DQ and newmark methods", *Comput. Concr.*, **19**(6), 745-753.
<https://doi.org/10.12989/cac.2017.19.6.745>
- Motezaker, M., Kolahchi, R., Rajak, D.K. and Mahmoud, S.R. (2021), "Influences of fiber reinforced polymer layer on the dynamic deflection of concrete pipes containing nanoparticle subjected to earthquake load", *Polym. Compos.*,
<http://doi.org/10.1002/pc.26118>.
- RabaniBidgoli, M. and Saeidifar, M. (2017), "Time-dependent buckling analysis of SiO_2 nanoparticles reinforced concrete columns exposed to fire", *Comput. Concr.*, **20**(2), 119-127.
<https://doi.org/10.12989/cac.2017.20.2.119>
- Safari Bilouei, B., Kolahchi, R. and Rabanibidgoli, M. (2016), "Buckling of concrete columns retrofitted with Nano-Fiber Reinforced Polymer (NFRP)", *Comput. Concr.*, **18**(5), 1053-1063. <https://doi.org/10.12989/cac.2016.18.6.1053>
- Shokravi M. (2017), "Vibration analysis of silica nanoparticles-reinforced concrete beams considering agglomeration effects", *Comput. Concr.*, **19**(3), 333-338.
<https://doi.org/10.12989/cac.2017.19.3.333>
- Simsek, M. (2010), "Non-linear vibration analysis of a functionally graded Timoshenko beam under action of a moving harmonic load", *Compos. Struct.*, **92**, 2532-2546.
<https://doi.org/10.1016/j.compstruct.2010.02.008>
- Su, Y., Li, J., Wu, C and Li, Z.X. (2016), "Influences of nanoparticles on dynamic strength of ultra-high performance concrete", *Compos. Part B Eng.*, **91**, 595-609.
<https://doi.org/10.1016/j.compositesb.2016.01.044>
- Taherifar, R., Zareei, S.A., Bidgoli, M.R. and Kolahchi, R. (2020), "Seismic analysis in pad concrete foundation reinforced by nanoparticles covered by smart layer utilizing plate higher order theory", *Steel Compos. Struct.*, **37**(1), 99-115.
<https://doi.org/10.12989/scs.2020.37.1.099>
- Yaylaci, M., Adiyaman, G., Oner, E., Birinci, A.J.S.E. and Mechanics (2020), "Examination of analytical and finite element solutions regarding contact of a functionally graded layer", *Struct. Eng. Mech.*, **76**(3), 325-336.

<http://doi.org/10.12989/sem.2020.76.3.325>.

Yoon, H.I. and Son, I. (2007), "Dynamic response of rotating flexible cantilever fluid with tip mass", *Int. J. Mech. Sci.*, **49**, 878-887. <https://doi.org/10.1016/j.ijmecsci.2006.11.006>

ZamaniNouri, A. (2017), "Mathematical Modeling of concrete pipes reinforced with CNTs conveying fluid for vibration and stability analyses", *Comput. Concr.*, **19**(3), 325-331. <https://doi.org/10.12989/cac.2017.19.3.325>

Zhai, H., Wu, Z., Liu, Y. and Yue, Z. (2011), "Dynamic response of pipeline conveying fluid to random excitation", *Nucl. Eng. Des.*, **241**, 2744-2749. <https://doi.org/10.1016/j.nucengdes.2011.06.024>

CC